Pergamon

Int. J. Heat Mass Transfer. Vol. 40, No. 13, pp. 3005–3012, 1997

Printed in Great Britain
0017-9310/97 $17.00+0.00

PII: S0017-9310(96)00371-7

Natural convection with unsaturated humid air in vertical cavities

G. D. McBAIN
Department of Mechanical Engineering, James Cook University of North Queensland, Townsville, QLD 4811, Australia

(*Received* 29 *April* 1996 *and in final form* 31 *October* 1996)

Abstract—Simple formulae for the overall heat and moisture transport rates due to laminar natural convection in a rectangular cavity are obtained by scale analysis from the governing differential equations and a simplified picture of the flow. The two formulae contain a single unknown proportionality constant, which is determined by a least squares fit to the results of a series of numerical solutions. The relations apply for the case of isothermal vertical walls at constant, unsaturated relative humidity, and adiabatic, impermeable horizontal walls. The heat transfer formula agrees well with published data for the square cavity with zero humidity gradient. © 1997 Elsevier Science Ltd.

INTRODUCTION

The transfer of heat by natural convection across vertical air filled cavities is important in assessing the thermal performance of buildings. The flow in an enclosure is driven by differences in density due to temperature and composition gradients. The most common compositional gradient is that due to humidity. A humidity gradient will also lead to the transfer of energy by desorption and adsorption which may, particularly in the tropics, far exceed the heat transfer. An understanding of these two effects of humidity on natural convection in vertical air filled cavities is thus crucial for the design of energy efficient housing in warm, humid climates.

If the humidity boundary conditions everywhere involve either saturation or impermeability, the problem may be solved with the Close–Sheridan analogy [1, 2] and any of the plentiful heat transfer only solutions [3–6]. This assumes the air to be everywhere saturated within the cavity, so that the thermodynamic state of the fluid at any point is uniquely determined by the total pressure and the temperature. The humidity transport equation is, thereby, rendered redundant. The vapour pressure exerted by a porous body, such as often forms a cavity boundary, is generally less than the saturation value [7], so that the state at any point within the cavity is a function of three independent intensive properties (e.g. total pressure, temperature and specific humidity). The humidity transport equation must, therefore, be retained, unless the thermal and compositional diffusivities are equal and the thermal and compositional boundary conditions are similar, allowing the solution of the problem using heat transfer only correlations. For moist air, the diffusivities are roughly equal ($Le \approx 0.85$), so that this approach may yield fairly accurate transport rates. In general, however, the humidity and transport equations are independent.

In the past, scale analysis has been used to predict the asymptotic behaviour of the transport rates in vertical boundary layers, as the Prandtl and Schmidt numbers tend to zero or infinity for buoyancy dominated by either temperature or concentration gradients [8]. These results have been verified numerically for the square cavity [9], but difficulties were encountered in the "transitional" region, i.e. Prandtl and/or Schmidt numbers around unity. Since for humid air, the Prandtl and Schmidt numbers are both of order unity, and the magnitudes of the thermal and compositional buoyancies are often comparable, this asymptotic analysis is of limited use. Further, while vertical boundary layers tend to form in the cavity as the buoyancy forces increase, the stagnation in the corners significantly affects the flow and consequent convective transport. This was also suggested by Béghein *et al.* [9], as a possible cause for their correlation difficulties. The effect is more pronounced at lower aspect ratios so that, for example, the approximate analytic solution of Raithby *et al.* [10] for the single fluid case is not expected to hold for $\mathscr{A} < 5$. In this paper, Prandtl and Schmidt numbers are just less than unity, as appropriate for humid air. Further, the effect of the corners is taken into account.

THE PROBLEM

For simplicity, we deal only with two dimensional, steady, laminar flows with no condensation within the flow field and negligible viscous dissipation, Soret and Dufour effects. The governing equations are thus [11]:

$$\nabla \cdot \rho \mathbf{u} = 0 \tag{1}$$

NOMENCLATURE

$\mathscr{A}$	cavity aspect ratio
Bo_v	virtual Boussinesq number, $\rho^2 c_p^2 g\beta_v \Delta T_v L^3/k^2$
Bo_v^*	mass transfer virtual Boussinesq number, $g\beta_{v\Delta} T_v L^3/D^2$
C	constant of proportionality
c_p	isobaric specific heat
D	binary diffusivity
g	gravitational field strength
$\hat{j}$	unit vertical vector
k	thermal conductivity
L	cavity width
Le	Lewis number, Sc/Pr
m	mass fraction of water vapour in humid air
M	molar mass
N	buoyancy ratio, $(\beta_v \Delta T_v/\beta \Delta T)-1$
Nu	Nusselt number, $q'/\mathscr{A}k\Delta T$
p	total pressure
p'	excess pressure, $p+\rho g y$
Pr	Prandtl number, μ/kc_p
q'	heat transfer rate per unit depth of cavity
$\mathscr{R}$	universal gas constant
Ra	Rayleigh number, $\rho^2 c_p g\beta \Delta T L^3/\mu k$
Sc	Schmidt number, $\mu/\rho D$
Sh	Sherwood number, ratio of mass transfer to that under pure diffusion
T	absolute temperature.

Greek symbols

β	bulk expansion coefficient
δ	characteristic diffusion length
Δ	difference, generally across cavity, but in (19)–(22) across vertical boundary layer
η	normalised longitudinal boundary layer coordinate
λ	characteristic advection length
μ	dynamic viscosity
ρ	density.

Subscripts

a	dry air
v	virtual
w	water vapour
0	reference level.

$$\rho \mathbf{u}\cdot\nabla\mathbf{u} = -\nabla p' - [\rho - \rho(T_0,0)]g\hat{j} + \nabla\cdot\mu\nabla\mathbf{u} + \tfrac{1}{3}\nabla\mu\nabla\cdot\mathbf{u} \quad (2)$$

$$\rho c_p \mathbf{u}\cdot\nabla T = \nabla\cdot k\nabla T \quad (3)$$

$$\rho\mathbf{u}\cdot\nabla m = \nabla\cdot\rho D\nabla m. \quad (4)$$

The density may be expressed in terms of the virtual temperature, defined as the temperature at which dry air would have the same density and total pressure [12]. Assuming that humid air behaves as an ideal gas mixture, this gives:

$$\rho = pM_a/\mathscr{R}T_v \quad (5)$$

$$T_v = T[1-(1-M_a/M_w)m]. \quad (6)$$

The boundary conditions commonly considered in single fluid studies are isothermal vertical walls and adiabatic horizontal walls. For the mass transfer, we extend these to constant humidity vertical walls and impermeable horizontal walls. The velocity is assumed to be zero at the walls. The situation is summarised in Fig. 1.

$$T(0,y) = T_0 - \Delta T/2, \quad T(L,y) = T_0 + \Delta T/2 \quad (7)$$

$$m(0,y) = m_0 - \Delta m/2, \quad m(L,y) = m_0 + \Delta m/2 \quad (8)$$

$$\left.\frac{\partial T}{\partial y}\right|_{y=0} = \left.\frac{\partial T}{\partial y}\right|_{y=H} = \left.\frac{\partial m}{\partial y}\right|_{y=0} = \left.\frac{\partial m}{\partial y}\right|_{y=H} = 0 \quad (9)$$

$$\mathbf{u} = 0, \quad x = 0, L \quad \text{and} \quad y = 0, H. \quad (10)$$

A SIMPLIFIED PICTURE OF THE FLOW FIELD

According to Gill's [13] picture of the flow in the single fluid case, the natural length scale of the flow is not the same everywhere in the cavity. The transport of momentum, heat and humidity occurs by advective and diffusive processes. Advection dominates where the local component of velocity parallel to the direction of interest is large. Following Gill, we assume that there exists a stagnant core which is stably stratified with respect to virtual temperature. Significant flow occurs only in the boundary layers along the walls, up the virtually hotter wall, down the virtually colder wall and horizontally at the other walls so as to make a single cell.

Thus transport will occur primarily by advection along and diffusion across the layers, and we can say that there are two characteristic lengths for the flow: one for diffusive processes, denoted by δ and related to the boundary layer thickness, and one for advection, λ, related to the boundary layer length. As the horizontal walls are adiabatic and impermeable, we need consider only the transport in the vertical boundary layers. Simplistically, we assume that λ and δ are independent of position and moreover apply equally to the transport of momentum, heat and humidity. This is only reasonable in so far as the Prandtl and Schmidt numbers are of order unity.

The advection length, λ, may be related to the cavity

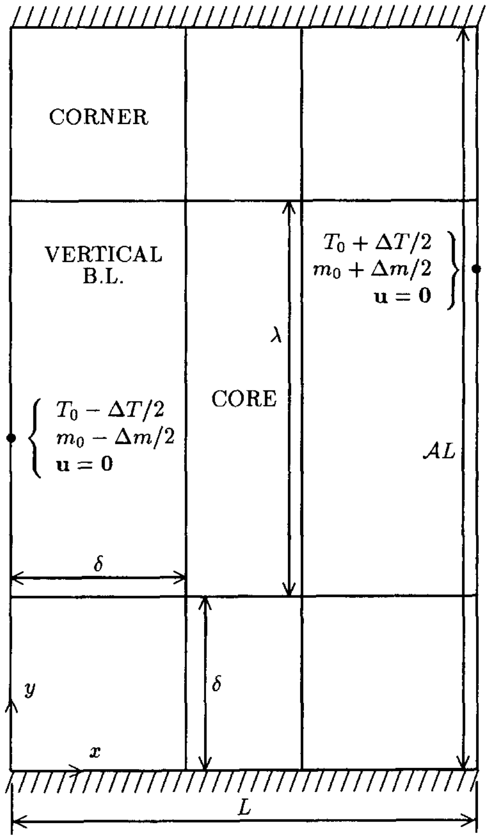

Fig. 1. The conceptual subdivision of the cavity, showing diffusion and advection lengths.

height, $\mathscr{A}L$, if we further assume that no significant transport occurs in the corner regions, and that the dimensions of these are of the same order as the diffusion length, δ. Thus,

$$\lambda \approx \mathscr{A}L - 2\delta. \tag{11}$$

The conceptual subdivision of the cavity is illustrated in Fig. 1.

SCALES IN THE VERTICAL BOUNDARY LAYERS

The Nusselt Number, Nu, is closely related to the ratio of the advection and diffusion lengths. For the actual heat transfer, neglect the corners, where the flow is stagnant and assume simple conduction across the hot wall boundary layer. Assume that the temperature in the core is linearly distributed from the minimum to the maximum values (the temperatures at the cold and hot walls, respectively) up the outside of the vertical boundary layers, so that the local temperature differences across the vertical boundary layers vary linearly from 0 to ΔT. The heat transfer rate for the cavity is then given by:

$$q' = \frac{k}{\delta}\lambda \int_0^1 (1-\eta)\Delta T \, d\eta$$

$$= \frac{k\Delta T \lambda}{2\delta}. \tag{12}$$

The pure conduction heat transfer is $\mathscr{A}Lk\Delta T/L = \mathscr{A}k\Delta T$, so that the Nusselt number is:

$$Nu = \frac{\lambda}{2\mathscr{A}\delta} \tag{13}$$

The Nusselt (or Sherwood) number for a vertical natural convection boundary layer has been shown to be inversely proportional to the boundary layer thickness [8, 9], but here the relationship is not so simple, as the advection length, λ, is a function of δ (11). It will be true in the limit as the boundary layer thickness tends to zero, but at least in the laminar region, the boundary layers account for a sizable portion of the total cavity. Equation (13) thus takes into account, in a rudimentary way, the stagnation effect of the corners.

The conservation of momentum equation (2) consists of advection, excess pressure gradient, viscosity and buoyancy terms. The excess pressure gradient, $\nabla p'$, only plays a role in the corner regions, so that in the vertical boundary layers a balance must be struck between the inertial and frictional forces on one hand and the driving buoyancy force on the other, yielding:

$$\text{Inertia} \quad \rho\left(u\frac{\partial v}{\partial x} + v\frac{\partial v}{\partial y}\right) \tag{14}$$

$$\text{Friction} \quad \mu\left(\frac{\partial^2 u}{\partial x \partial y} + \frac{\partial^2 v}{\partial x^2} + \frac{4}{3}\frac{\partial^2 v}{\partial y^2}\right) \tag{15}$$

$$\text{Buoyancy} \quad (\rho - \rho_0)g. \tag{16}$$

According to the discussion of the previous section, the operator $\partial/\partial y$ should be replaced by $1/\lambda$ and $\partial/\partial x$ by $1/\delta$ and their operands by the relevant characteristic scale. If we assume $\lambda \gg \delta$ and $v \gg u$ (hence limiting attention to the boundary layer regime) and neglecting bulk expansion and property variations (as is routinely done in the Boussinesq approximation), the magnitudes of the inertia and friction terms are of order:

$$\text{Inertia} \quad \rho V^2/\lambda \tag{17}$$

$$\text{Friction} \quad \mu V/\delta^2 \tag{18}$$

where V is the as yet undetermined vertical speed scale.

Rewriting the buoyancy term as the first two terms of a Taylor series expansion in the virtual temperature, according to the full (ideal) equation of state:

$$\rho - \rho_0 = -\beta_v \Delta T_v \rho_0 \tag{19}$$

where

$$\beta_v \equiv 1/T_{v0} \tag{20}$$

$$T_{v0} \equiv T_0[1-(1-M_a/M_w)m_0]. \quad (21)$$

Thus, the buoyancy term becomes:

$$\text{Buoyancy} \quad g\beta_v \Delta T_v \rho. \quad (22)$$

ΔT_v in equation (22) refers to the virtual temperature difference across the vertical boundary layer. This varies with height (decreasing up the virtually hotter wall) because of the stratification of the core, but in an average sense will be proportional to the difference between the two vertical walls. This is the meaning with which we invest ΔT_v from now on so this only gives a prediction for the overall transport rate, not the local values.

The use of the single variable, the virtual temperature, T_v, to characterise the buoyancy force implicitly assumes that the compositional and thermal boundary layers are of similar thickness. Equation (3) requires a balance between conduction across the boundary layer and advection along it, hence:

$$\frac{\rho c_p V}{\lambda} \sim \frac{1}{\delta^2} \quad (23)$$

where both temperature gradients have been assumed to be proportional to the temperature difference across the cavity and, therefore, each other. This can be solved to express the speed scale in terms of the characteristic lengths:

$$V \sim \frac{k\lambda}{\rho c_p \delta^2} \quad (24)$$

and hence, by equations (11) and (13) (dropping the pure number, 2), in terms of the Nusselt number, fluid properties and cavity dimensions:

$$V \cdot \frac{L}{k/\rho c_p} \sim Nu(Nu+\mathscr{A}^{-1}). \quad (25)$$

This aptness of this speed scale is investigated later, via the results of the numerical solutions. Equation (24) can be substituted into the inertia and friction scales (17) and (18):

$$\text{Inertia} \quad \frac{k^2\lambda}{\rho c_p^2 \delta^4} \quad (26)$$

$$\text{Friction} \quad \frac{\mu k \lambda}{\rho c_p \delta^4}. \quad (27)$$

The balance between inertia, friction and buoyancy now reads [14]

$$\frac{k^2\lambda}{\rho c_p^2 \delta^4}\left[1+O\left(\frac{\mu c_p}{k}\right)\right] \sim \rho g \beta_v \Delta T_v \quad (28)$$

or, multiplying through by L^3 and introducing the Prandtl and virtual Boussinesq numbers,

$$\frac{L^3 \nu}{\delta^4} \sim \frac{Bo_v}{1+O(Pr)}. \quad (29)$$

Between equations (11), (29) and (13), the characteristic lengths can be eliminated to give a proportionality relating the heat transfer rate to the boundary conditions and fluid properties.

$$Nu(Nu+\mathscr{A}^{-1})^3 \sim \frac{Bo_v}{\mathscr{A}[1+O(Pr)]} \quad (30)$$

As the Prandtl number for humid air is relatively constant, it is not possible to accurately determine the precise dependency, so here we replace $O(Pr)$ with simply Pr and insert an undetermined proportionality constant, to give the equation

$$\frac{Bo_v}{\mathscr{A}(1+Pr)} = C\,Nu(Nu+\mathscr{A}^{-1})^3. \quad (31)$$

SCALE ANALYSIS OF THE HUMIDITY TRANSPORT

Because the species equation (4) is formally identical to the heat equation (3), the final result of the previous section may be carried over, with the obvious substitution of the Sherwood number for the Nusselt number, the Schmidt number for the Prandtl number, and a modified virtual Boussinesq number,

$$\frac{Bo_v^*}{\mathscr{A}(1+Sc)} = C\,Sh(Sh+\mathscr{A}^{-1})^3. \quad (32)$$

VERIFICATION AGAINST NUMERICAL SOLUTIONS

That the constant, C, should be the same in both cases, or even that it should be constant, cannot be proved *a priori*, as so many assumptions have been made along the way. To resolve this question, the formulae were tested against a series of numerical simulations, performed on the finite element fluid dynamics package, FIDAP† [15]. The numerical solutions allowed testing of both the predictions for the overall transport rates and the scaling rules employed.

A total of 45 runs were made for a 50 mm square cavity filled with air at mean temperatures from 10 to 50°C, with a 5 K temperature difference and the vertical walls having equilibrium relative humidities of 0, 50 and 100%. The equations solved were (1)–(4) above. The fluid property data used is shown in Table 1. All runs were made at a constant total pressure of 101, 325 Pa. Further details of the solutions are given in Ref. [16]. The dimensionless correlation parameters were evaluated at the arithmetic mean temperature and specific humidity.

The speed scale is validated in Fig. 2, where the maximum vertical speed from each run is used. The figure shows that the relation (25) is well represented by a linear equation:

†The rights to use FIDAP have been acquired by the Department of Mechanical Engineering under license from Fluid Dynamics International.

Table 1. Fluid property data used in the 45 FIDAP runs. The transport properties were evaluated at each node by linear interpolation in the intensive variable (in the left column of each subtable) between the values listed. The saturation specific humidity was evaluated only at the temperatures shown, for the vertical wall boundary condition. The data are from Professor D. J. Close (pers. comm.)

T (°C)	k (mW/m.K)	D (mm²/s)	μ (μPa.s)	m_{sat} ($\times 10^3$)
5.0	24.5	—	17.5	5.4
7.5	—	—	—	6.4
10.0	24.9	23.4	17.7	—
12.5	—	—	—	9.0
17.5	—	—	—	12.3
20.0	25.6	24.7	18.1	—
22.5	—	—	—	16.9
27.5	—	—	—	22.9
30.0	26.4	26.3	18.6	—
32.5	—	—	—	30.6
37.5	—	—	—	40.6
40.0	27.3	28.0	19.0	—
42.5	—	—	—	53.4
47.5	—	—	—	69.8
50.0	28.2	29.5	19.3	—
52.5	—	—	—	90.4
60.0	29.1	30.9	19.6	—

m (—)	c_p (J/kg.K)
0.0	1004
7.7	1010
15.3	1016
23.1	1022
30.9	1028
38.8	1034
46.8	1040
54.8	1046
63.0	1052
71.2	1058
79.5	1065

$$\frac{VL\rho c_p}{k} = 2.82Nu(Nu+\mathscr{A}^{-1}) \qquad (33)$$

for which the rms relative error is 2.0%.

The proportionality constant, C, is determined to be 53.5 by a least squares fit of equation (31) to the numerical heat transfer results (see Fig. 3). The resulting curve, along with $\pm 5\%$ accuracy limits, is shown for the Nusselt and Sherwood numbers in Figs 4 and 5, respectively.

If the proportionality constant had been determined instead by a regression to the mass transfer data, it would have differed by less than 0.2%. As the coefficient acts on a fourth degree polynomial of the Nusselt or Sherwood number, the corresponding error in the transfer rates is substantially less. This is a striking verification of the handling of the heat and mass transfer analogy and the use of the virtual temperature in the scale analysis.

All the points with $Bo_v > 10^4(1+Pr)$ or $Bo_v^* > 10^4(1+Sc)$ agree with the formula to within 5%. For lower virtual Boussinesq numbers, the quantitative agreement is only fair, as presumably the boundary layer approximations are less appropriate.

VERIFICATION AGAINST PUBLISHED DATA FOR THE DRY AIR CASE

Equation (31) should be applicable to the problem of the dry air cavity, noting that the virtual temperature reduces to the normal temperature in this case. To test this, the correlation is compared with de Vahl Davis' bench mark solution for a single, Boussinesq fluid of $Pr = 0.71$ in a square cavity [5], by plotting (see Fig. 6) the bench marks points and the curve

$$Ra = 53.5\frac{1+Pr}{Pr}Nu(Nu+\mathscr{A}^{-1})^3. \qquad (34)$$

The agreement is excellent (better than 2%) for the points at $Ra = 10^4$, 10^5 and 10^6, which is very encouraging, particularly as it represents an extrapolation outside the range of the data used in determining the proportionality coefficient, the highest (virtual) Rayleigh number used in the numerical solutions was 1.9×10^5.

The equation is out by 12% for the $Ra = 10^3$ case (when the boundary layer approximations are least valid). As Gill [13] gives the criterion for distinct

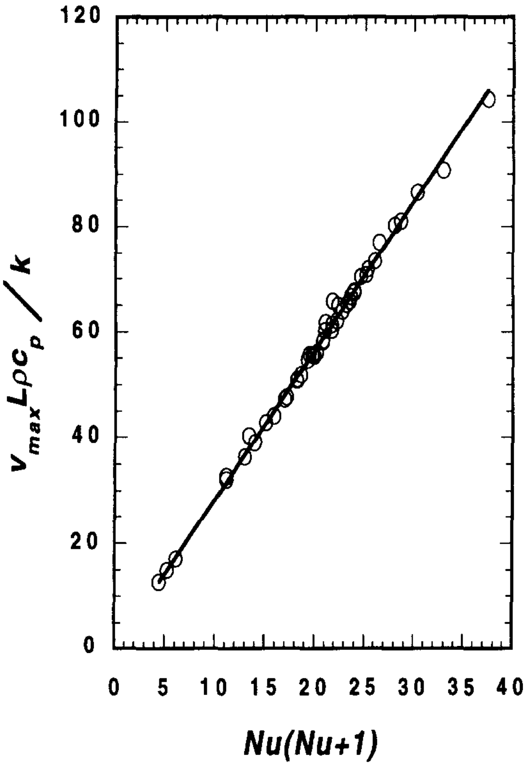

Fig. 2. Demonstration of the validity of the speed scale (24). The speed, v_{max}, used is the maximum nodal vertical component of velocity from each of the 45 FIDAP solutions. The curve is a least squares slope of best fit: $y = 2.32x$.

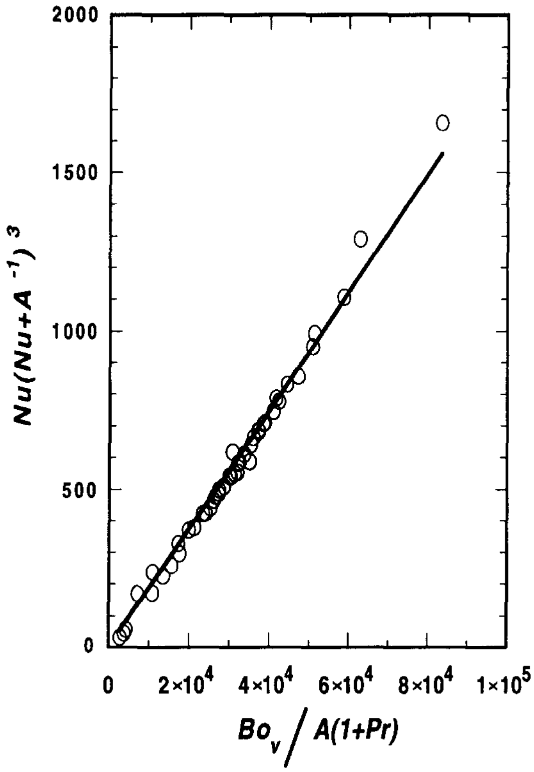

Fig. 3. Demonstration of the validity of the heat transfer proportionality (30). Determination of the proportionality constant by slope of best fit.

boundary layers as $Ra > 2\times10^4$, even this level of agreement is surprisingly good. Predicting a Nusselt number less than unity is unreasonable however, though in this lower Rayleigh number range, the heat transfer is little higher than the $Nu = 1$ level, so that the performance of the formula is of no practical importance.

DISCUSSION

Relative to the virtual Boussinesq number, the Nusselt number appears in equation (30) as a fourth degree polynomial. Such a relation could not be revealed by a log–log plot. However, it may be significant that the index of the Rayleigh number is often reported in the literature as being somewhere between 1/4 and 1/3. For example, Chenoweth and Paolucci [6] give 0.2969 as the value for $\mathscr{A} = 1$. The tall cavity ($\mathscr{A} > 5$) approximate analytic solution reported by Raithby *et al.* [10] contains a 1/4 power dependence, though they note that this is not to be expected for lower aspect ratio cavities. Equation (31) behaves in this way, approaching a simple one-fourth power law as the aspect ratio increases.

The proportionality cannot be expected to hold at very low virtual Boussinesq numbers because, in this case, from equation (29), the "boundary layers" must meet in the middle, eliminating the core. The model

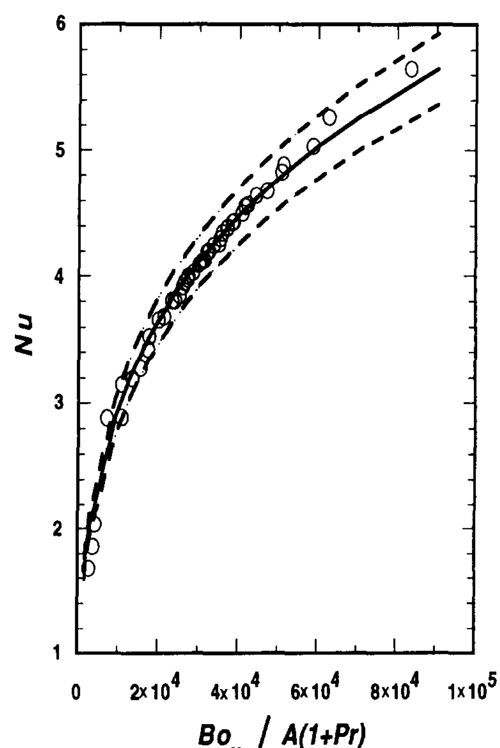

Fig. 4. Heat transfer; points are the results from the 45 FIDAP tests. The solid curve is equation (31) and the $\pm5\%$ error region is included.

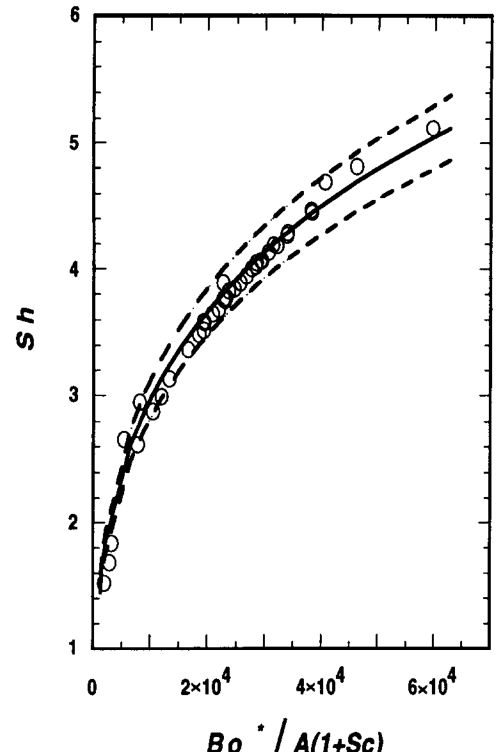

Fig. 5. Mass transfer. Points are the results of the 40 FIDAP tests with non-zero humidity gradients. The solid curve is equation (32), with the proportionality constant, $C = 54.5$, obtained from the heat transfer results in Fig. 3; the dashed curves represent $\pm 5\%$ accuracy limits.

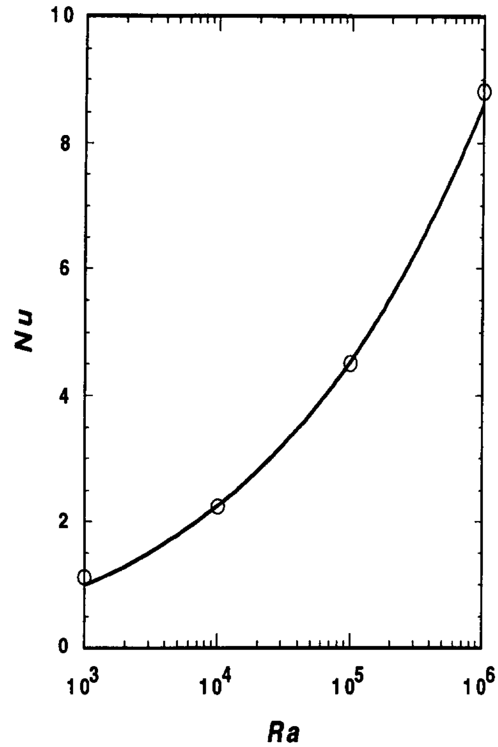

Fig. 6. Comparison of the present scale analysis, the curve is equation (34), with de Vahl Davis' bench mark solution [5] for the square cavity with no humidity gradient (the points).

does take account of the reduction in the size of the core when the boundary layers are not insignificantly thin, but not to this extent. In the limit as the virtual Boussinesq number goes to zero, the Nusselt number should approach unity, as the heat transfer takes place by pure conduction. The proportionality does not do this. The 45 tests extend down to virtual Boussinesq numbers around 4000. A rough guide to the lower limit of applicability of the model is obtained by substituting $Nu = 1$ into equation (31), which gives $Bo_v = 435(1+Pr)$ for the square cavity, the analysis is clearly invalid for lower Boussinesq numbers and improves to better than $\pm 5\%$ accuracy as $Bo_v > 10^4(1+\mathrm{Pr})$.

If the momentum balance against the bouyancy force had been taken with either the inertia or friction singly, the heat transfer equation (30) would contain either the Boussinesq or Rayleigh number, with no Prandtl number dependency. This corresponds to the asymptotic behaviour as the Prandtl tends to zero or infinity. The natural convection heat transfer correlations of LeFevre [17], Berkovsky and Polevikov [4] and Rohsenhow and Choi [18] display the same asymptotic behaviour, though all four interpolation formulae differ. The range of Prandtl numbers in the present work ($0.7 < Pr < 0.821$) is not really wide enough to pick up the distinctions, though the Schmidt number is lower (down to 0.605), so that the importance of obtaining the correct dependency arises in the use of the same formal equation for the heat and mass transfer. Stating that C is the same in the two equations (31) and (32) means:

$$\frac{f(Sh)}{f(Pr)} = \frac{Bo_v^*(1+Pr)}{Bo_v(1+Sc)} \tag{35}$$

where $f(x) = x(x+\mathscr{A}^{-1})^3$. If this is correct, the ratio of the estimates for C from the mass transfer data and heat transfer data would be

$$\frac{Pr(1+Sc)}{Sc(1+Pr)} \tag{36}$$

if the inertial force were neglected. This ratio is 1.10 for $Pr = 0.71$ and $Sc = 0.61$. If the friction force were neglected, the ratio would be

$$\frac{1+Sc}{1+Pr} \tag{37}$$

which is 0.94. These ratios compare poorly with the 0.998 obtained by the present analysis.

By the similarity of the heat and mass transfer equations, the Sherwood number should be the same function of the Schmidt number as the Nusselt is of the Prandtl number, which is supported by the present results. Both the Nusselt and Sherwood numbers, however, should depend on both the Prandtl and Schmidt numbers. This has been ignored here, as the Lewis number is close to unity. Physically this crossdependence results from the different influence of compositional and thermal gradients on the buoyancy when the relevant boundary layers differ appreciably in extent, i.e. the virtual temperature would no longer be sufficient to describe the buoyancies, and the results would vary with the buoyancy ratio, N, a parameter that was ignored in the scale analysis. That this causes no serious error for humid air can be judged by the accuracy of the predictions, given that a wide spread of the buoyancy ratio is covered by the 45 FIDAP runs: $-2.7 < N < 3.5$. If the Lewis number were further from unity, the buoyancy ratio could be expected to increase in importance.

CONCLUSION

Theoretically based formulae for the total, steady state heat and mass transfer rates across vertical cavities have been obtained. The single adjustable constant has been found by regression to numerical solutions. The formulae have been tested against numerical solutions for a square cavity involving a wide range of humidity gradients. The formulae worked well, with the bulk of the points lying within the $\pm 5\%$ range, with poorest performance occurring for very low virtual Boussinesq numbers (in the conduction/diffusion regime). The results have not been tested for aspect ratios other than unity and do not include three-dimensional or transient effects. No turbulent flows were studied.

Acknowledgments—The author would like to thank Professor D. J. Close, Dr H. Suehrcke and Dr J. A. Harris for many critical and informative discussions, technical assistance and generally creating and maintaining an excellent research environment. The work presented in this paper forms a part of a larger study on heat and mass transfer which is being supported by the Australian Research Council.

REFERENCES

1. Close, D. J. and Sheridan, J., Natural convection in enclosures filled with a gas and a non-condensing gas. *International Journal of Heat and Mass Transfer*, 1989, **32,** 855–862.
2. Close, D. J., Peck, M. K., White, R. F. and Mahoney, Buoyancy-driven heat transfer and flow between a wetted heat source and an isothermal cube. *Journal of Heat Transfer, Transactions of ASME*, 1991, **113,** 371–376.
3. Jakob, M., *Heat Transfer*. Wiley, New York, 1949, pp. 538–539.
4. Berkovsky, B. M. and Polevikov, V. K., Numerical study of problems in high-intensive free convection. In *Heat Transfer and Turbulent Buoyant Convection* (ed. D. B. Spalding and H. Afghan). Hemisphere, Washington, D.C., 1977, pp. 443–455.
5. de Vahl Davis, G., Natural convection of air in a square cavity: a bench mark numerical solution. *International Journal of Numerical Methods Fluids*, 1983, **3,** 249–264.
6. Chenoweth, D. R. and Paolucci, S., Natural convection in an enclosed vertical air layer with large horizontal temperature differences. *Journal of Fluid Mechanics*, 1986, **169,** 173–210.
7. Defay, R., Prigogine, I. and Bellemans, A., *Surface Tension and Adsorption*, English edn, translated by D. H. Everett. Longmans, London, 1966, p. 223.
8. Bejan, A., *Convection Heat Transfer*, 2nd edn. Wiley, New York, 1995, pp. 490–494.
9. Béghein, C., Haghighat, F. and Allard, F., Numerical study of double-diffusive natural convection in a square cavity. *International Journal of Heat and Mass Transfer*, 1992, **35,** 833–846.
10. Raithby, G. D., Hollands, K. G. T. and Unny, T. E., Analysis of heat transfer by natural convection across vertical fluid layers. *Journal of Heat Transfer, Trans. ASME*, 1977, **99,** 287–292.
11. Bird, R. B., Stewart, W. E. and Lightfoot, E. N., *Transport Phenomena*, Ch. 10. Wiley, New York, 1960.
12. Rogers, R. R. and Yau, M. K., *A Short Course in Cloud Physics*, 3rd edn. Pergamon, Oxford, 1989, p. 17.
13. Gill, A. E., The boundary layer regime for convection in a rectangular cavity. *Journal of Fluid Mechanics*, 1966, **26,** 515–536.
14. Suehrcke, Dr H., Personal communication, 10 February, 1996.
15. FIDAP Version 7.51, Fluid dynamics analysis package, Fluid Dynamics International, 500 Davis St, Suite 600, Evanston, IL, 1995.
16. McBain, G. D., The effect of humidity on natural convection in vertical air filled cavities. Bachelor of Engineering thesis, Department of Mechanical Engineering, James Cook University of North Queensland, Townsville, Queensland, 1995.
17. LeFevre, E. J., Laminar free convection from a vertical plane surface. *Proceedings of the Ninth International Congress of Applied Mechanics*, Vol. 4, 1957, pp. 168–174.
18. Rohsenhow, W. M. and Choi, H. Y., *Heat, Mass and Momentum Transfer*. Prentice-Hall, Englewood Cliffs, New Jersey, 1961, p. 159.